2012

Raman And X-Ray Photoelectron Spectroscopy Study Of Ferroelectric Switching In Pb(Nb,Zr,Ti)O3 Thin Films

E. Ramos-Moore

P. Ferrari

D. E. Diaz-Droguett

D. Lederman

J. T. Evans

AIP Journal of Applied Physics

Raman and x-ray photoelectron spectroscopy study of ferroelectric switching in Pb(Nb,Zr,Ti)O3 thin films

E. Ramos-Moore, P. Ferrari, D. E. Diaz-Droguett, D. Lederman, and J. T. Evans

Citation: Journal of Applied Physics **111**, 014108 (2012); doi: 10.1063/1.3675479
View online: http://dx.doi.org/10.1063/1.3675479
View Table of Contents: http://scitation.aip.org/content/aip/journal/jap/111/1?ver=pdfcov
Published by the AIP Publishing

Raman and x-ray photoelectron spectroscopy study of ferroelectric switching in $Pb(Nb,Zr,Ti)O_3$ thin films

E. Ramos-Moore,[1,a)] P. Ferrari,[1] D. E. Diaz-Droguett,[1] D. Lederman,[2] and J. T. Evans[3]
[1]*Facultad de Física, Pontificia Universidad Católica de Chile, Santiago 7820436, Chile*
[2]*Multifunctional Materials Laboratory, Department of Physics, West Virginia University, Morgantown, West Virginia 26506-6315, USA*
[3]*Radiant Technologies, Inc., Albuquerque, New Mexico 87106, USA*

(Received 11 October 2011; accepted 8 December 2011; published online 9 January 2012)

The ferroelectric switching process in $Pb(Nb,Zr,Ti)O_3$ thin films was studied by performing Raman spectroscopy and x-ray photoelectron spectroscopy (XPS). Switching was achieved using a macroscopic polarization experiment above and below the Curie temperature. Two samples in opposite switching states were obtained and characterized in order to correlate both vibrational-bands distortions of the bulk and changes in the elemental states of the surface. We have assigned the symmetrical $A_1(2TO)$ (332 cm^{-1}) and $A_1(3TO)$ (603 cm^{-1}) vibrational modes to the ferroelectric phase. Their corresponding peaks-area showed symmetrical behavior when the sample was polarized in opposite directions, while the quantity of phonons associated to the ferroelectric phase was conserved. We found that binding energies in the XPS signals of the Ti 2p, Nb 3d, Zr 3d, and Pb 4f levels increased when comparing to the values found in a non-polarized sample. Moreover, a high population of oxygen vacancies diffused to the surface of the ferroelectric capacitor under the application of external electric fields. Our novel results show the correlation between vibrational and ferroelectric behaviors and highlight the possibility to perform *in situ* treatments to decrease the degradation of current technological capacitors. © *2012 American Institute of Physics*. [doi:10.1063/1.3675479]

I. INTRODUCTION

Ferroelectric thin films based on lead zirconate titanate (PZT) are considered[1] as the most promising candidates for non-volatile memories and related applications. Their properties rely in the ability to displace the zircon and titanium ions at the octahedral site of the PZT-perovskite into one of the symmetric potential wells along the polarization axis. The small metal ions can be switched between these two states by applying external electric fields higher than the coercive field (~100 kV/m), leading to a gradual inversion of the macroscopic polarization. This model[2] is usually called "rattling titanium" and although is well accepted for bulk materials, new models need experimental evidence in order to validate the surface/bulk phenomena, since the film thickness decrease.[3–5] In fact, the model does not consider relevant issues such as retention loss, charge injection, and depolarizing fields, which are mainly related with the presence of oxygen vacancies at the electrode/ferroelectric interfaces.[6,7]

On the other hand, the manipulation of ferroelectric domains at the surface of thin films has also motivated several studies[8–11] that have explored surface reactivity for gas sensing and related applications. Among others, we can mention photochemical oxidation and reduction of ferroelectric domains,[12] surface potential screening due to gas adsorption,[11] modification of ferroelectric performance due to presence of oxygen vacancies,[13] and interstitial hydrogen.[14] Moreover, we have recently demonstrated[15] the controlled generation of oxygen vacancies in the surface of $Pb(Nb,Zr,Ti)O_3$ (PNZT) thin films.

In this work, we performed polarization experiments by applying positive and negative voltages below and above the Curie temperature (T_C), in order to study the correlation of bulk and surface phenomena in PNZT domains inversion. Two samples in opposite switching states were obtained and characterized by Raman and x-ray photoelectron spectroscopy (XPS) in order to study the vibrational-bands distortions of bulk and changes in the elemental states of the surface, respectively.

II. EXPERIMENT DESCRIPTION

The samples used in this study consisted of 4% niobium doped 20/80 PZT thin films (200 ± 15 nm) provided by Radiant Technologies Inc. and grown at 650 °C by metal–organic deposition on the substrate $Pt/TiO_2/SiO_2/Si$. The lateral sample size was ~1 cm^2. Previous x-ray diffraction measurements[15] performed at room temperature showed the presence of (100), (110), and (111) planes that correspond to the pervoskite structure in the tetragonal (ferroelectric) phase. Before the experiment, the samples were annealed at 650 °C for 2 h using O_2 flux. This standard procedure allows the filling of oxygen vacancies and diffusion of interstitial hydrogen, thus achieving better stoichiometry.

The switching setup was similar to the one used by Li *et al.*[11] Two PNZT samples ($E^{\pm}$) were macroscopically polarized by applying ±10 V (± 500 kV/cm) between the

a)Electronic mail: evramos@fis.puc.cl.

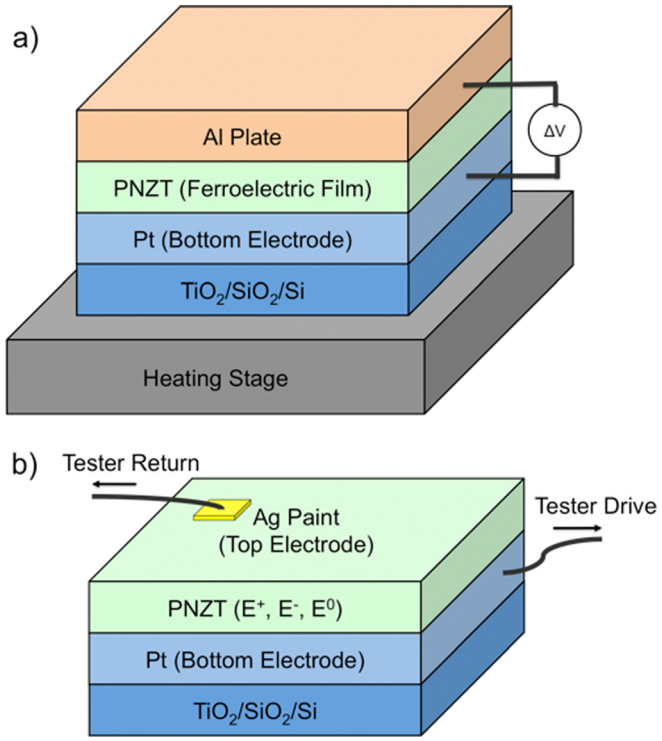

FIG. 1. (Color online) (a) Experimental setup used in the polarization experiment. Between the Al plate and the bottom electrode, ±10 V ($E^{\pm}$) were applied while heating the sample in air up to 600 °C for 30 min. (b) Experimental setup for measuring the ferroelectric parameters were characterized for E^+, E^-, and a non-polarized sample (E^0).

bottom electrode (Pt) and a polished plate (Al) placed on top of the sample, as shown in Fig. 1(a). While the voltage was applied, each sample was heated from room temperature to 600° at 20 °C/min, which corresponds to ~150 °C above the Curie temperature T_C. After 30 min of annealing, the sample was cooled back using the same rate. For comparison purposes, a third sample (E^0) was also annealed in the absence of external voltages. As shown in Fig. 2, positive (negative) charge was induced in the PNZT top surface of the E^+ (E^-) sample during the experiment, and thus, the structure was expected to freeze in both ferroelectric states once cooled to room temperature.

After the experiment, the flat plate was removed in order to perform ferroelectric, Raman and XPS characterization. As shown in Fig. 1(b), the commercial ferroelectric tester RT66B (Radiant Technologies Inc.) was used to characterize the ferroelectric behavior by connecting the bottom electrode to the tester output (drive) and the top electrode (Ag paint) to the tester input (return). In order to measure the charge per area (polarization), the current was integrated in steps of 100 ms. The area of the top electrode was 0.02 cm^2.

The surface chemical information was obtained from XPS using a Physical Electronics system model 1257, equipped with a Mg Kα x-ray source (1253.6 eV). The binding energies (BE) were obtained from high-resolution scans (pass energy 71.55 eV and step size 0.2 eV). The energy scale was calibrated by assigning the 284.8 eV peak to the C_{1s} peak.

Non-polarized Raman spectra were obtained with a LabRam 010 instrument from ISA using a 5.5 mW He–Ne laser (632.8 nm). The scanned area was 1 $\mu m \times 1$ μm, and the energy resolution was 1.07 cm^{-1}. A Linkam TMS 94 controller and THMS 600 stage were used to vary the sample temperature with a precision of 0.1 °C.

III. RESULTS AND ANALYSIS

A. Ferroelectric characterization

Ferroelectric hysteresis loop measurements were carried out in the ±9.9V range. The remanent polarization was determined by measuring the normal hysteresis loop before and after domain inversion by switching the sign of the previous preset pulse. Subtraction of the loops corresponds to the value of the accumulated charge per area due to ferroelectric domain inversion only.

Figure 3 shows the room temperature hysteresis loop and remanent hysteresis measured in the Ag/PNZT/Pt capacitor using the non-polarized PNZT sample (E^0). The saturation of polarization was 3.3 (−4.0) $\mu C/cm^2$, the remanent polarization was 1.6 (−1.6) $\mu C/cm^2$, and the coercive voltage was 4.5 (−7.2) V. Thus, fields higher than 225 (−360) kV/cm ensure external polarization. Although similar samples[16,17] have shown saturation values higher than 10$\mu C/cm^2$, we measured lower values due to the low efficiency of the painted-on electrode that is contacting the surface at few

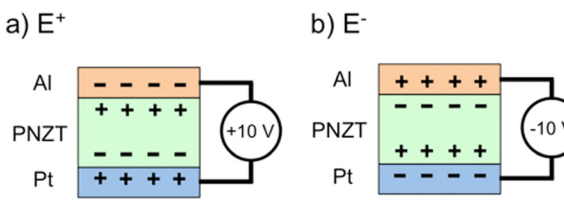

FIG. 2. (Color online) Electric scheme of the polarization experiment when applying (a) +10 V (E^+) and (b) −10 V (E^-) between the top and bottom electrodes.

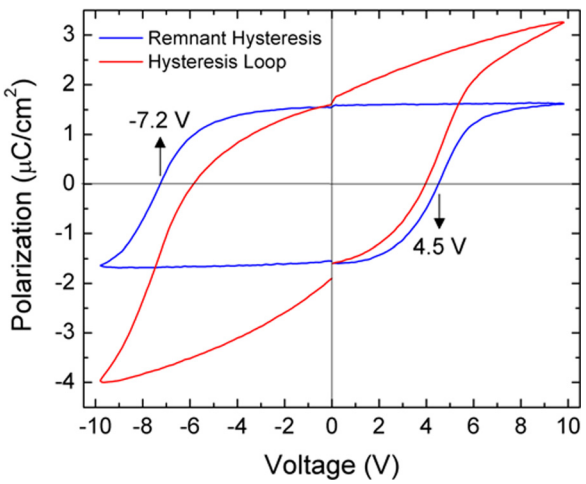

FIG. 3. (Color online) Room temperature hysteresis loop and remanent hysteresis measured in the Ag/PNZT/Pt capacitor using the non-polarized PNZT sample (E^0). The coercive voltages indicated in the graph by the arrows were calculated from the remanence data.

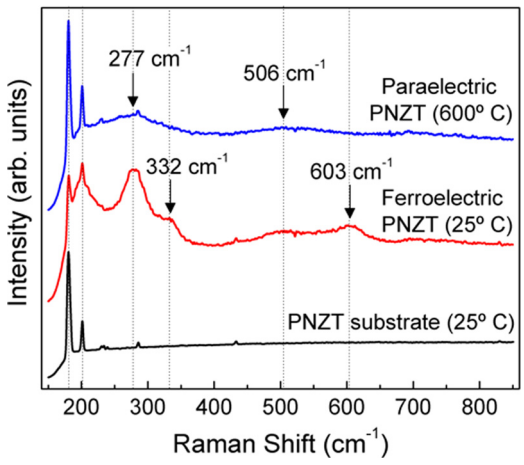

FIG. 4. (Color online) Raman spectra of the substrate ($Pt/TiO_2/SiO_2/Si$), ferroelectric PNZT at 25 °C, and paraelectric PNZT at 600 °C. The peaks associated with the substrate below 200 cm^{-1} are present in all three samples.

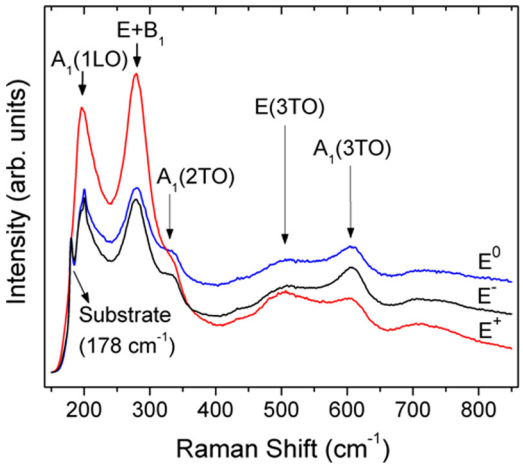

FIG. 5. (Color online) Raman spectra at room temperature of the non-treated (E^0) and polarized ($E^{\pm}$) PNZT samples, normalized to the substrate peak at 178 cm^{-1}. The ferroelectric peaks at 332 cm^{-1} ($A_1(2TO)$) and 603 cm^{-1} ($A_1(3TO)$) showed different intensities in $E^{\pm}$ compared to E^0.

points to achieve adhesion. The non-symmetric values of the coercive voltages might correspond to the difference between the work functions of the Ag and Pt electrodes.[18,19] According to the literature,[20] the difference between the work functions of Ag and Pt is 1.39 V, and the loop shifted 1.37 V toward negative values of voltages. The difference (0.02 V) might be explained by a depletion shift at the PNZT/Pt interface after annealing.

B. Raman spectroscopy

Figure 4 shows the spectra obtained for the substrate ($Pt/TiO_2/SiO_2/Si$) at room temperature and PNZT at 25 °C and 600 °C. The peaks associated with the substrate below 200 cm^{-1} were present in all three samples. The PNZT room temperature scan had peaks characteristic of the tetragonal ferroelectric phase at 332 cm^{-1} and 603 cm^{-1}. In the high-temperature spectrum these peaks were absent. Peaks at 277 cm^{-1} and 506 cm^{-1} represent the paraelectric behavior of the structure. According to the normal modes description[21,22] of PZT, the Raman spectrum at room temperature corresponds to the point group symmetry C_{4V} associated with a tetragonal structure, and the Raman active vibrations correspond to A_1, B_1, and E modes. Although Nb doping might modify the phonon dispersion,[23] we focus on the study of bands associated with the ferroelectric phase, as determined by comparing spectra below and above T_C (Fig. 4).

Figure 5 shows the Raman spectra of a non-treated (E^0) and polarized ($E^{\pm}$) PNZT samples. The active Raman bands correspond to $A_1(1LO)$, $E+B_1$, $A_1(2TO)$, E(3TO), and $A_1(3TO)$, as designated by Burns and Scott[24,25] and agree with recent measurements performed on similar films.[26] The peaks corresponding to the ferroelectric phase were associated to the $A_1(2TO)$ (332 cm^{-1}) and $A_1(3TO)$ (603 cm^{-1}) bands. Both modes had different intensities in the $E^{\pm}$ samples when compared to the E^0 sample, and slight changes were also observed in the $A_1(1LO)$, $E+B_1$, and E(3TO). To the best of our knowledge, these data are the first evidence of a correlation between structural distortion and the vibrational spectrum of PNZT thin films.

In order to quantify the effect of polarization on the vibrational spectrum, a Gaussian fit was performed according to the modes description of Frantti and Lantto.[27] Figure 6 summarizes the fit of the Raman spectra in Fig. 5 after linear subtraction and compares the peak-area of the paraelectric ($E+B_1$ and E(3TO)) and ferroelectric ($A_1(2TO)$ and $A_1(3TO)$) peaks for the unpolarized (E^0) and polarized ($E^{\pm}$) PNZT samples. For vibrations at low (high) frequencies, which generally correspond to heavy (light) atom movements, we observed a ferroelectric/paraelectric ratio of 0.40 (0.63) in E^-, 0.45 (0.56) in E^0, and 0.50 (0.50) in E^+. For all the fitted data, we observed statistical errors in peak-area ratios lower than 0.02.

From the reduced data we first note that the peak-area ratio $A_1(2TO)/E+B_1$ decreases (increases) the same amount as the ratio $A_1(3TO)/E(3TO)$ when the sample was negatively (positively) polarized, thus the quantity of phonons corresponding to the ferroelectric phase is constant. Second, the shift in the area-ratio value is 0.05 (−0.07) between E^- and E^0, and 0.05 (−0.06) between E^0 and E^+, thus indicating a symmetrical distribution of the quantity of the corresponding phonons.

C. X-ray photoelectron spectroscopy

Figure 7 shows XPS survey spectra of the PNZT films. Figure 7(a) is the reference spectrum acquired from the non-polarized film (E^0). Figure 7(b) is the spectrum of the sample with positive polarization (E^+) and Fig. 7(c) corresponds to the sample with negative polarization (E^-).

The intensities ratios among the photoelectron signals of the spectra 7(a) and 7(b) are very similar. Both spectra show the photoelectron peaks of Pb (Pb4p, Pb4d, Pb4f, Pb5d), O (O1s), Ti (Ti2p, Ti3p), Zr (Zr3s, Zr3p, Zr3d), and Nb (Nb 3d). The C1s photoelectron peak corresponds to the adventitious carbon on the surface. In contrast, the photoelectron signals associated to Pb, Ti, Zr, and Nb are not detected in the spectrum 7(c) corresponding to the E^- sample. The BE of the main signal associated to these elements is indicated

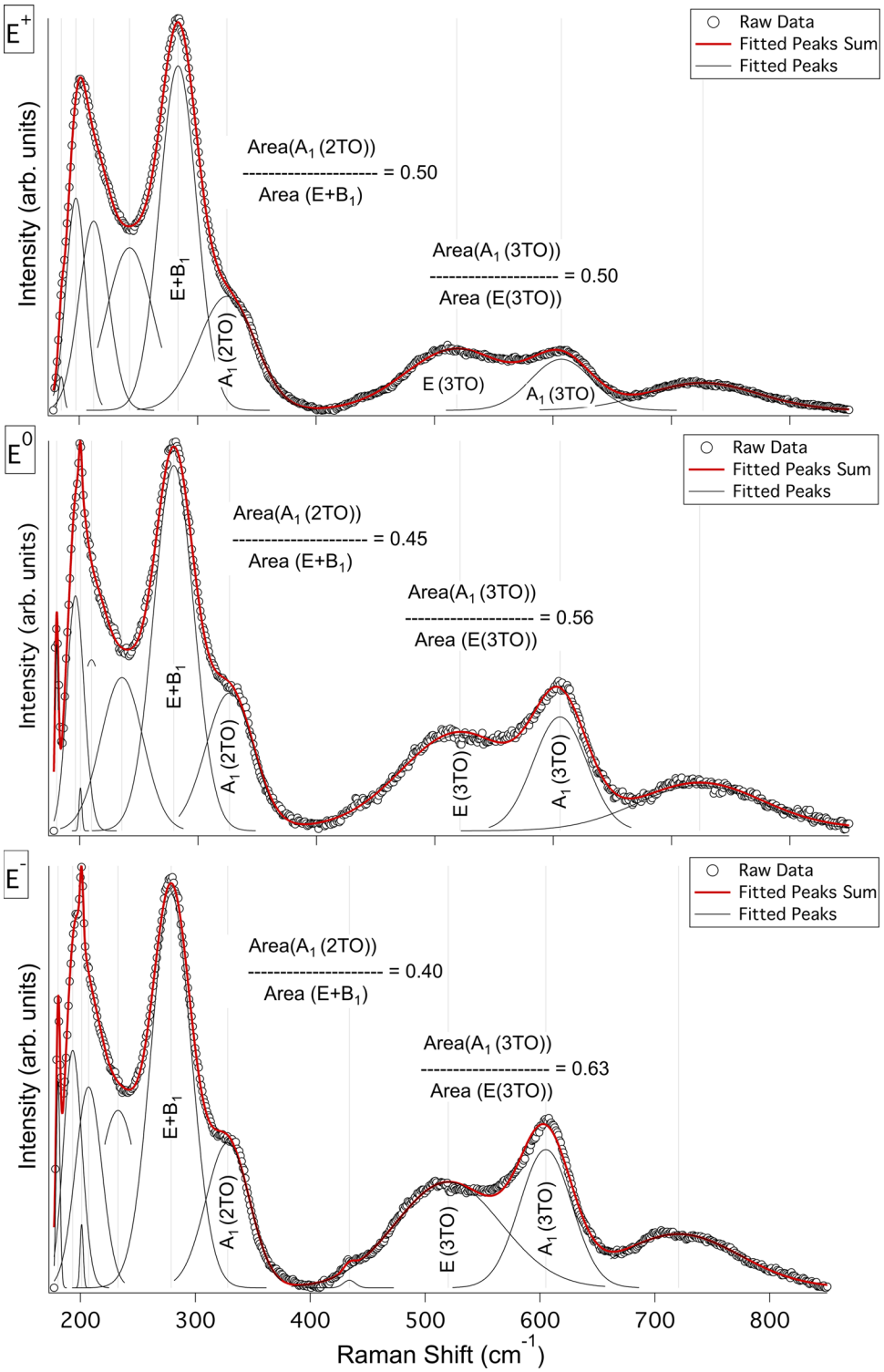

FIG. 6. (Color online) Gaussian peaks fit of the Raman spectra showed in Fig. 5, after subtraction of a linear background. Raw data are in gray markers. The areas of the ferroelectric (A_1(2TO) and A_1(3TO)) and paraelectric ($E+B_1$ and E(3TO)) peaks were compared for the unpolarized (E^0) and polarized ($E^{\pm}$) PNZT samples.

by an arrow in Fig. 7(c). It is worth mentioning that the Pb4f peak is the strongest signal in the spectra 7(a), and Fig. 7(b) is slightly detectable for the E^- sample. The spectrum 7(c) presents another important difference due to its strong intensity of the C 1s peak compared with the O 1s peak, since the intensities ratio (I_{C1s}/I_{O1s}) is close to 1, while 0.4 and 0.6 for E^0 and E^+, respectively. As shown in Fig. 2, the accumulation of negative charge in the surface of the film may induce carbon and oxygen adsorption from the ambient.

The *ex situ* polarization effect on the oxygen vacancies distribution of the PNZT films is clearly evidenced in the high-resolution XPS spectra of the O 1s signal. Figure 8 shows high-resolution XPS spectra of the O1s signal and its corresponding curve fitting of the PNZT films. Figure 8(a) shows the spectrum acquired from the non-polarized sample, and Figs. 8(b) and 8(c) are the spectra of the samples polarized as E^+ and E^-, respectively. The fit of the spectrum 8(a) was resolved using two peaks where the binding energy (BE)

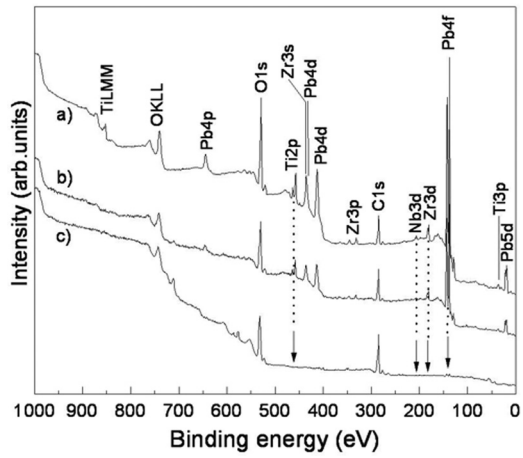

FIG. 7. XPS survey spectra of the PNZT films: (a) E^0, (b) E^+, and (c) E^-. The signals associated with Pb, Ti, Zr, and Nb were detected for all except the E^- sample due to the high amount of oxygen and adventitious carbon adsorbed.

of the highest intensity (curve I) corresponds to oxygen in the PNZT lattice, including Pb-O, Ti-O, Zr-O, and Nb-O bonding whereas the binding energy of the lower intensity (curve II) was attributed[28,29] to the presence of oxygen vacancies and hydroxyl (OH) groups on the film surface. A fit for distinguishing between peaks corresponding to oxygen vacancies and OH groups was not possible. The fit of this spectrum assigned a BE of 529.0 eV and a full width at half maximum (FWHM) of 1.4 eV to oxygen in the PNZT lattice and 531.1 eV and a FWHM of 2.2 eV to oxygen vacancies and OH groups. These BEs are close to reported values of 529.0 eV for oxygen in PNZT and 532.0 eV for oxygen vacancies and OH groups.[30] The spectra of the polarized samples, Figs. 8(b) and 8(c), needed an additional peak for their fits. As the previous case, the curve I and curve II were associated to the oxygen in the PNZT lattice and to oxygen vacancies plus OH groups, respectively. The third peak (curve III) was attributed to the presence of H_2O adsorbed on the film surface. It has been found[31] that the BE of the oxygen in H_2O adsorbed on oxide film is major than the BE associated to OH groups. The BEs associated to the curve III were found at 533.2 eV (FWHM 2.3 eV) and 532.8 eV (FWHM 2.3 eV) for the sample with positive and negative polarization, respectively, as shown by Figs. 8(b) and 8(a). The BE attributed to oxygen in PNZT lattice (curve I) was of 529.4 eV (FWHM 1.6 eV) and 529.8 eV (FWHM 1.6 eV) for the E^+ and E^- sample, respectively. A shift toward BEs higher of 0.4 eV for the E^+ sample and a shift of 0.8 eV for the E^- sample compared with the values found for the non-polarized sample. On the other hand, the BE associated to oxygen vacancies and OH groups (curve II) was found at 531.4 eV (FWHM 2.4 eV) and 531.5 eV (FWHM 2.1 eV) for the samples with positive and negative polarization, respectively. The shape of the O1s signal from the spectra 8(a) and 8(b) were similar except by the slight shoulder associated to the curve III in 8(b). However, the O1s signal of the E- sample shows that the peak with the highest intensity was associated to oxygen vacancies and OH groups (curve II), as

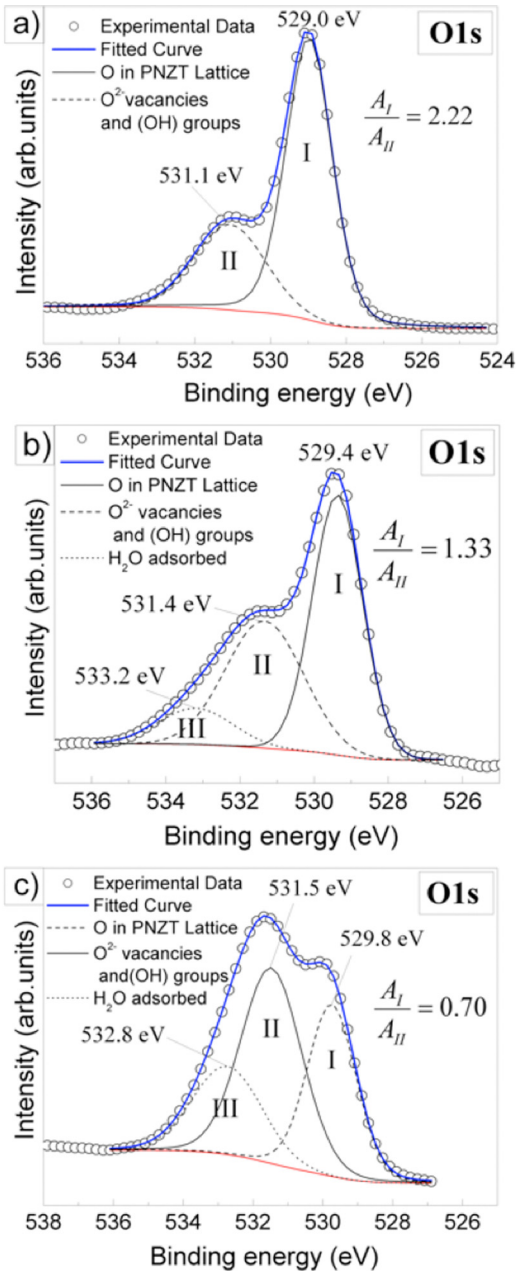

FIG. 8. (Color online) High-resolution XPS spectra of the O1s signal corresponding to (a) E^0, (b) E^+, and (c) E^-. Curve I corresponds to oxygen in the PNZT lattice, curve II was attributed to the presence of oxygen vacancies and hydroxyl (OH) groups, and curve III was attributed to the presence of H_2O adsorbed in the film surface.

shown in Fig. 8(c). The ratio between the areas below the curves I and II, A_I/A_{II}, calculated for all the spectra was of 2.22, 1.33, and 0.70 for the non-polarized, E^+ sample and E^- sample, respectively. The low ratio and the high intensity of the curve II (III) for the E^- (E^+) sample are attributed to a major concentration of oxygen vacancies (water) in the film surface. The *ex-situ* negative polarization on this film caused the diffusion of the O^{2-} vacancies of the as-prepared sample toward the surface, which it was in contact with the positive electrode. In this context, the surface state goes into equilibrium with the air by emitting oxygen to create more oxygen vacancies, which then diffuse into the film. This process

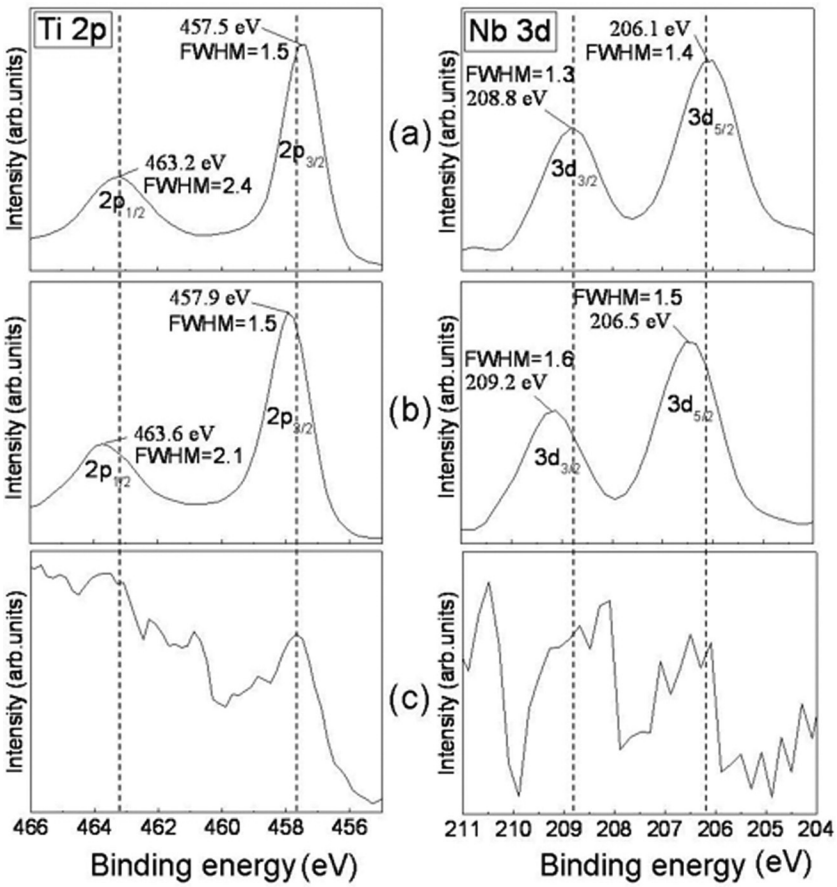

FIG. 9. High-resolution XPS spectra of the Ti 2p and Nb 3d signals corresponding to the (a) E^0, (b) E^+, and (c) E^- samples.

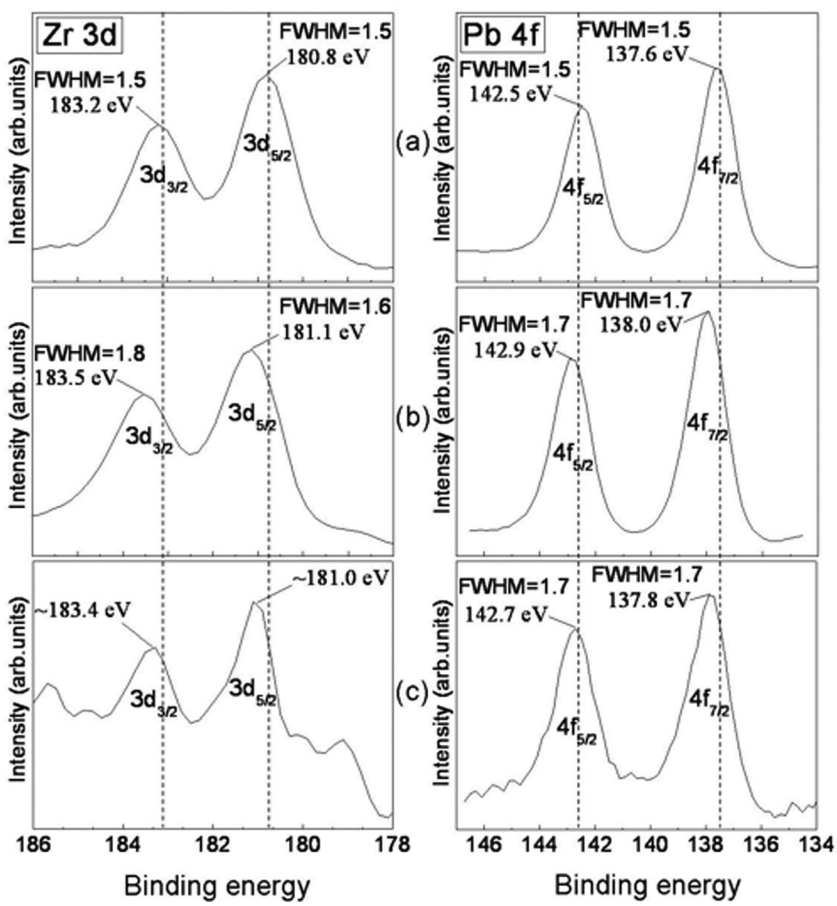

FIG. 10. High-resolution XPS spectra of the Zr 3d and Pb 4f signals corresponding to the (a) E^0, (b) E^+, and (c) E^- samples.

represent a "pump" that fills up the capacitor volume with oxygen vacancies that after saturation, starts to degrade.[32] Hence, the opposite voltage polarization makes the capacitors more reliable by filling oxygen vacancies and might eventually increase the performance of oxide barriers currently used in top[16] and bottom[26] PNZT electrodes.

Figure 9 shows high-resolution XPS spectra of the Ti 2p and Nb 3d signals acquired from each sample: (a) E^0, (b) E^+, and (c) E^-. The BEs as well as the FWHM values for each level are indicated in the figures. The BEs of the Ti $2p_{3/2}$ and $2p_{1/2}$ levels are close to the reported values for PNZT film.[30] The Ti 2p and Nb 3d signals of E^0 and E^+ samples have the same spectral shape. A shift of 0.4 eV toward higher BEs of the Ti 2p and Nb 3d levels was detected between these samples, as indicated by dotted lines in the spectra pair of Figs. 9(a) and 9(b). The low signal/noise ratio in the Ti 2p and Nb 3d signals for E^- shown in Fig. 9(c) is produced by the screening of these signals due to the higher abundance of oxygen and carbon, as shown in the survey spectrum in Fig. 7.

Figure 10 shows high-resolution XPS spectra of the Zr 3d and Pb 4f signals. The BEs and the FWHM values of the different levels are indicated in the spectra. The BEs of the Zr 3d and Pb 4f levels for the non-polarized sample are close to the reported values for PNZT films.[30] A shift of the polarized samples toward higher BEs was also detected when compared with the values of the non-polarized sample, as indicated by the vertical dotted lines in Fig. 10. Although low signal/noise ratio is still found in the spectral shape of the Zr 3d and Pb 4f signals acquired from the non-polarized and E^+ sample (Fig. 10(c)), both remain similar to the signals acquired from the E^- sample. We note that the shift of Nb (0.4 eV), Zr (0.3 eV), and Ti (0.4 eV) peaks of the E^+ and E^- samples is similar. The shift in Pb (0.4 eV) indicates that Pb ions at the surface also participate in the ferroelectric switching process. This agrees with prior work on PNZT thin films, which shows poor reliability under Pb excess and polarization suppression under Pb deficiency.[33]

IV. CONCLUSIONS

We have characterized the ferroelectric properties of PNZT thin films poled with the electric field parallel and antiparallel to the surface normal. From Raman scattering we have identified ferroelectric and paraelectric vibrational modes and their corresponding bands. The shifts of the ferroelectric/paraelectric peaks-area ratio were similar when the sample was polarized either negatively or positively and the quantity of phonons corresponding to the ferroelectric phase stays constant.

Analysis of XPS data indicate that water is adsorbed when applying positive voltages to the top electrode during annealing, whereas oxygen vacancies are generated when applying negative voltages. Hence, a high population of oxygen vacancies diffused toward the positive electrodes. This type of sample treatment is proposed to enhance the reliability of PNZT thin films by filling oxygen vacancies at the electrode/ferroelectric interface. Moreover, the ability to localize the oxygen vacancies leads to charge accumulation at specific region of the capacitor, the same as p-type doping in silicon or charge injection in a metal–oxide–semiconductor field-effect transistor (MOSFET). A shift of the peaks corresponding toward higher BEs was detected in Ti 2p, Nb 3d, Zr 3d, and Pb 4f photoelectron signals of the polarized samples with respect to the values found in the non-polarized sample. The increase in BE of the Nb 3d and Pb 4f levels suggests that presence of Pb and Nb ions is also relevant in the switching process at the surface.

Finally, we note that the understanding of the correlation between bulk and surface phenomena in ferroelectric thin films is crucial to develop future applications not only in the field of electronics, but also in gas sensing and catalysis.

ACKNOWLEDGMENTS

We would like to thank the Facultad de Física at Pontificia Universidad Católica de Chile for financial support. Work at WVU was supported in part by the Office of Naval Research and the National Science Foundation.

[1]N. Izyumskaya, Y. I. Alivov, S. J. Cho, H. Morkoç, H. Lee, and Y. S. Kang, Critical Rev. Solid State Mat. Sci. **32**, 111 (2007).
[2]Y. Ishibashi, *Ferroelectric Thin Films* (Springer-Verlag, New York, 2005).
[3]J.-E. Lim, D.-Y. Park, J. K. Jeong, G. Darlinski, H. J. Kim, C. S. Hwang, S.-H. Kim, C.-Y. Koo, H.-J. Woo, D.-S. Lee, and J. Ha, Appl.Phys. Lett. **81**, 3224 (2002).
[4]C. H. Ahn, Science **303**, 488 (2004).
[5]P. Aguado-Puente and J. Junquera, Phys. Rev. Lett. **100**, 177601 (2008).
[6]K. T. Li and V. C. Lo, J. Appl. Phys. **97**, 034107 (2005).
[7]M. Grossmann, O. Lohse, D. Bolten, U. Boettger, and R. Waser, J. Appl. Phys. **92**, 2688 (2002).
[8]Y. Yun, L. Kampschulte, M. Li, D. Liao, and E. I. Altman, J. Phys. Chem. C **111**, 13951 (2007).
[9]M. H. Zhao, D. A. Bonnell, and J. M. Vohs, Surf. Sci. **603**, 284 (2009).
[10]E. Ramos-Moore, J. A. Baier-Saip, and A. L. Cabrera, Surf. Sci. **600**, 3472 (2006).
[11]D. Li, M. H. Zhao, J. Garra, A. M. Kolpak, A. M. Rappe, D. A. Bonnell, and J. M. Vohs, Nature Mater. **7**, 473 (2008).
[12]J. L. Giocondi and G. S. Rohrer, J. Phys. Chem. B **105**, 8275 (2001).
[13]J. F. Scott and M. Dawber, Appl. Phys. Lett. **76**, 3801 (2000).
[14]S. Aggarwal, S. Perusse, C. Tipton, and R. Ramesh, Appl. Phys. Lett. **73**, 1973 (1998).
[15]E. Ramos-Moore, D. E. Diaz-Droguett, P. Spring, J. T. Evans, and A. L. Cabrera, Appl. Surf. Sci. **257**, 4695 (2011).
[16]R. Ramesh, G. Velasquez, L. Boyer, and J. Evans, Jr., Appl. Phys. Lett. **75**, 1787 (1999).
[17]C. E. Zybill, M. Abdel-Hafiez, S. Allam, and T. El Sherbini, Prog. Solid State Chem. **35**, 469 (2007).
[18]J. Rodríguez Contreras, H. Kohlstedt, U. Poppe, R. Waser, C. Buchal, and N. A. Pertsev, Appl. Phys. Lett. **83**, 4595 (2003).
[19]G. W. Dietz, W. Antpöhler, M. Klee, and R. Waser, J. Appl. Phys. **78**, 6113 (1995).
[20]D. R. Lide and H. P. R. Frederikse, *Handbook of Chemistry and Physics* (CRC, Boca Raton, 1994), p. 2608.
[21]K. Byrappa and T. Ohachi, *Crystal Growth Technology* (William Andrew, New York, 2003), p. 590.
[22]J. Lappalainen, J. Frantti, J. Hiltunen, V. Lantto, and M. Kakihana, Ferroelectrics **335**, 149 (2006).
[23]I. El-Harrad, P. Becker, C. Carabatos-Nédelec, J. Handerek, Z. Ujma, and D. Dmytrow, J. Appl. Phys. **78**, 5581 (1995).
[24]G. Burns and B. Scott, Phys. Rev. Lett. **25**, 1191 (1970).
[25]G. Burns and B. Scott, Phys. Rev. B **7**, 3088 (1973).
[26]Z.-X. Zhu and J.-F. Li, Appl. Surf. Sci. **256**, 3880 (2010).
[27]J. Frantti and V. Lantto, Phys. Rev. B **56**, 221 (1997).

[28]K. Nonaka, M. Akiyama, T. Hagio, and A. Takase, Jpn. J. Appl. Phys. **34**, 2344 (1995).
[29]T.Yu, Y.-F. Chen, Z.-G. Liu, S.-B. Xiong, L. Sun, X.-Y. Chen, and N.-B. Ming, Mater. Lett. **26**, 291-294 (1996).
[30]Q. Zou, H. Ruda, B. G. Yacobi, and M. Farrell, Thin Solid Films **402**, 65 (2002).
[31]D. E. D. Droguett, private communication (August 25, 2010).
[32]G. Y. Yang, G. D. Lian, E. C. Dickey, C. A. Randall, D. E. Barber, P. Pinceloup, M. A. Henderson, R. A. Hill, J. J. Beeson, and D. J. Skamser, J. Appl. Phys. **96**, 7500 (2004).
[33]S. Aggarwal, S. Madhukar, B. Nagaraj, I. G. Jenkins, R. Ramesh, L. Boyer, and J. T. Evans, Appl. Phys. Lett. **75**, 716 (1999).